International Journal of Innovative Technology and Exploring Engineering (IJITEE)
ISSN: 2278-3075 (Online), Volume-9 Issue-1, November 2019

Adaptive Unified Differential Evolution Algorithm for Optimal Operation of Power Systems with Static Security, Transient Stability and SSSC Device

B. Venkateswarlu, K.Vaisakh

Abstract*: The environmental degradation and increased power demand has forced modern power systems to operate at the closest stability boundaries. Thereby, the power systems operations mainly focus for the inclusion of transient stability constraints in an optimal power flow (OPF) problem. Algebraic and differential equations are including in non-linear optimization problems formed by the transient stability constrained based OPF problem (TSCOPF). Notably, for a small to large power systems solving these non-linear optimization problems is a complex task. In order to achieve the increased power carrying capacity by a power line, the Flexible AC transmission systems (FACTS) devices provides the best supported means a lot. As a result, even under a network contingency condition, the security of the power system is also highly improved with FACTS devices. The FACTS technology has the potential in controlling the routing of the line power flows and the capability of interconnecting networks making the possibility of trading energy between distant agents. This paper presents a new evolutionary algorithm for solving TSCOPF problems with a FACTS device namely adaptive unified differential evolution (AuDE). The large non-convex and nonlinear problems are solved for achieving global optimal solutions using a new evolutionary algorithm called AuDE. Numerical tests on the IEEE 30-bus 6-generator, and IEEE New England 10-generator, 39-bus system have shown the robustness and effectiveness of the proposed AuDE approach for solving TSCOPF in the presence of a FACTS device such as the SSSC device. Due to the page limitation only 30-bus results are presented.

Keywords: Adaptive unified differential evolution, power system transient stability, power system operation, power system security, optimal power flow

I. INTRODUCTION

One of the complex systems having more number of interconnected network transmission lines and generating units is known to be the power systems. However, the demands of huge electricity make the systems to operate their power transmission lines exceeding its prefixed limits (stability limits) and the power generation units [1, 2]. In case, if the system suffers from contingency or a fault then, the above said situations become so incredible and unsafe. Furthermore, the system tends to face voltage instability problem (sudden fall or rise of voltage) with the presence of fault or contingency disturbances. Consequently, voltage collapse is the final result achieved with the sudden fall or rise of system voltage. Sustaining less quality of service (QoS) loss during handling high and sudden disturbances defines the power system security [3]. Even though, the system after facing certain kinds of disturbances can ensure high transient stability while on maintaining proper planning and operation. Moreover, the system components when operated within their prefixed limits will allow the system to survive an acceptable equilibrium state [4].

Presently, the power system issues are better handled with the introduction of many advanced emerging technologies. Among these technologies, the flexible AC Transmission system (FACTS) is a popular one. Essentially, the Static Synchronous Series compensator (SSSC) is a commonly known type of FACTs device. A voltage in series with the line can be built effectively using this SSSC device. Also, the impedance changes in transmission lines are well regulated through inserting this SSSC device. Some of the crucial factors such as enhancement in power flow transfer capability, load bus voltage deviations, and power loss in the transmission lines were solved easily using this FACTs device [1-4].

Most of the past researchers have considered building the OPF model with transient stability constraints is a challenging and complex task. Two main steps included in the iterative process of TSC-OPF are as follows: Initially, the stability of system under contingency and with given equilibrium point is verified through conducting the transient stability analysis process. If system instability is caused with multiple or single contingency, then set of stability constraints are computed using the simulation outcomes [5-6]. Secondly, the newly improved operating condition is determined through using the formulation of optimal power flow with transient stability constraints. The first process known as transient stability analysis is repeated again for verifying the stability state of newly initialized operating condition (i.e. whether it has been stabilized already or not).

Revised Manuscript Received on November 30, 2019.
***** Correspondence Author
B. Venkateswarlu, Head of Electrical and Electronics Engineering, Department of Technical Education, Andhra Pradesh, Vijayawada,India Email: venkatbandi95@gmail.com
K. Vaisakh*, Department of Electrical Engineering, AU College of Engineering(A), Andhra University, Visakhapatnam,-530003 A.P, INDIA. Email: vaisakh_k@yahoo.co.in

Iteration of this two-step process is continued till satisfying the transient stability constraints by an equilibrium point [7-11].

Up-to-date, the classification of TSC-OPF is done in global or sequential manner after analyzing the ability of optimization problem in handling the stability constraints [12, 13].

Based on the classical OPF constraints, the direct representation of transient stability constraints is performed in sequential method. Then, the optimization program similar to traditional OPF or the classical OPF is used to implement the TS-OPF [14]. Conversely, the sequential methods in the presence of huge salient parameters can also show the transparency and computational efficiency while on using the classical OPF formulation. But, these methods have less ability to achieve the global optimal solution with minimum convergence time [15, 16].

TSCOPF problem can be solved through applying the evolutionary algorithms (EAs) to further withstand the limitations of gradient based techniques [17-20]. Typically, EAs are free from derivative complexities and they adopt the biological species related stochastic searching characteristics. EAs do not demand for any models complex differentiability or convexity requirements to determine the global optimal solution. Works in [21-23] has included the EAs namely, differential evolution (DE), particle swarm optimization (PSO), and genetic algorithm (GA) to solve the TS-OPF problems. In ten-generator New England system [21], the TSCOPF problem is solved effectively by means of applying an orthogonal array based genetic algorithm. Under multiple contingencies, the TSCOPF problem was solved using 'constriction factor PSO' commonly known as PSO variant in [22]. Work in [23] has attained a satisfactory solution through implementing a DE algorithm.

Global optimal solutions can be searched effectively using the differential evolution (DE) algorithm of Storn and Price [24]. Work in [25] has suggested that, when compared to EAs the DE is simpler and has showed better performance. In DE, five different types of mutation strategies were proposed by Storn and Price [26]. The mutation operation properties have been improved using various new mutation strategy variants [27]. But, the implementation of DE algorithm becomes so complex with the usage of various mutation operation strategies.

In this work, the global optimization process is done using the proposed adaptive unified differential evolution (AuDE) algorithm. This algorithm has encompassed all used mutation strategies by means of applying alone a single expression of mutation. Compared to other existing algorithms, the mathematical operation of AuDE algorithm becomes simple further with the usage of multiple mutation strategies. In the optimization process, various new combinations of existing mutation strategies are explored by the users enabled using multiple mutation strategies. The proposed AuDE becomes self-adaptive while on using the crossover and mutation operation and its control parameters. Furthermore, during the optimization process, this allows the users to select an optimal set of control parameters.

The paper is organized as follows. Inadequacies of existing methods are dealt using DE in TSCOPF problems. The computation of voltage stability index is given in Section II. The overview of the FACT device such as the SSSC device is given in Section III. The evaluation of static security index using fuzzy logic is given in Section IV. The formulation of TSCOPF problem is given in Section V. The overview of standard differential evolution is given in Section VI. The overview of the proposed adaptive unified differential evolution is given Section VII. The implementation steps of the AuDE algorithm for TSCOPF problem are given Section VIII. The AuDE based TSCOPF is studied on two test systems in Section IX using the 6-generator, IEEE 30-bus system and 10-generator, IEEE 39-bus system. Finally, Section X concludes the paper.

II. COMPUTATION OF VOLTAGE STABILITY INDEX (L-INDEX)

In normal operating conditions, each bus maintaining suitable levels of bus voltages defines the voltage stability of a power system. The power system enters into voltage instability condition when it is being subjected to different disturbances (system configuration changes, increase in load demand). Thereby, the uncontrollability in voltage reduction is experienced with these significant changes. As a result, one of the major tasks considered during power system operation is the good voltage stability maintenance in a power system. Proximities of voltage collapse condition are specified by the L-index of a bus. Equation (4.1) indicates the bus j^{th} corresponding L-index L_j condition [28].

$$L_j = \left|1 - \sum_{i=1}^{h} F_{ji} \frac{V_i}{V_j}\right| \text{ where } j = g+1,...,n \quad (1)$$

$$F_{ji} = -[y_1]^{-1}[y_2] \quad (2)$$

Number of load bus is indicated as N_{PQ} and number of PV bus is denoted as N_{PV}. The PQ and PV of the buses are separated to obtain y_1 and y_2 sub matrices of the YBUS system. It is indicated in Equation (3)

$$\begin{bmatrix} I_{PQ} \\ I_{PV} \end{bmatrix} = \begin{bmatrix} Y_1 & Y_2 \\ Y_3 & Y_4 \end{bmatrix} \begin{bmatrix} V_{PQ} \\ V_{PV} \end{bmatrix} \quad (3)$$

For all load buses, the voltage stability L-index is computed. Stable and no load case in a system is represented when L_j is closer to '0'. For bus 'j', the voltage collapse condition is determined when L_j is closer to 1, respectively. Equation (4) indicates the complete systems corresponding global stability indicator (L)

$$L = \max(L_j), \quad \text{where } j = 1,2,...,NPQ \quad (4)$$

A stable system is identified with least 'L' value. In a system, the voltage instability will be experienced with increased L-index values when tuned the control variables of the OPF problem solutions.

III. FACTS DEVICES

Power networks operations are well handled using the series of FACTs device. Furthermore, the FACTs devices can be used to enhance the power system stability and power system performance. The SSSC generates a series voltage which acts as a compensating voltage over both an inductive and capacitive range irrespective of the current flowing in the line.

SSSC controls can be used to vary rapidly the compensating voltage series corresponding phase and magnitude [29, 30]. In reality, the sensitivity of different buses will be different to the total voltage stability or power system performance. It is evident that, the voltage stability or power system performance can be improved greatly using SSSC [31, 32].

A. SSSC Device

Improved system performance is achieved through changing the parameters of power system network using the series of FACTs controllers. Enhanced reliability or security of the system and its dynamic behavior are the advantageous enjoyed using FACTs devices. Controlling the transmission lines during power flows is considered to be the main role of FACTs devices [33, 34]. In modern power system control and operation, these control characteristics have played an important role in FACTs devices. Figure 1 indicates the components of SSSC device such as, a capacitor, a coupling transformer and an inverter. Using a coupling transformer line, the power transmission lines are connected in series altogether with SSSC device. Usually, the reactance or impedance changes in the transmission line can be regulated through inserting or generating a series voltage using SSSC device. Likewise, the point at which the connection of SSSC is made can be used to control effectively the bus voltage or transmission line flows [35].

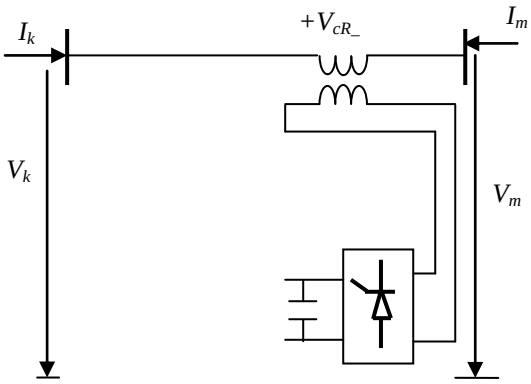

Figure 1a: Operating principle of SSSC

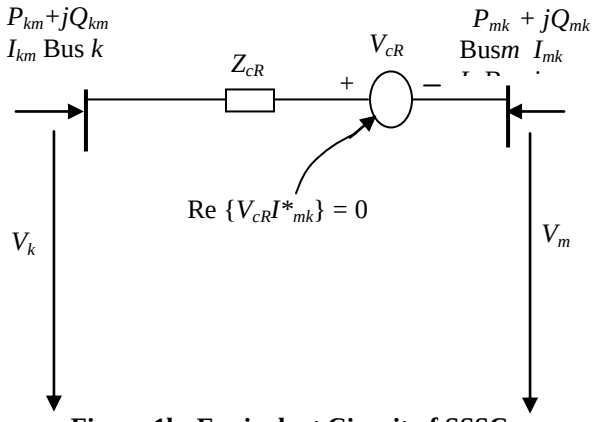

Figure 1b: Equivalent Circuit of SSSC

The equivalent circuit of SSSC is as shown in the Figure 1b. From the equivalent circuit the power flow constraints of the SSSC can be given as

$$P_{km} = V_k^2 g_{kk} - V_k V_m (g_{km}\cos\theta_{km} + b_{km}\sin\theta_{km}) - V_k V_{cR}(g_{km}\cos(\theta_k - \theta_{cR}) + b_{km}\sin(\theta_k - \theta_{cR})) \quad (5)$$

$$Q_{km} = -V_k^2 b_{kk} - V_k V_m (g_{km}\sin\theta_{km} + b_{km}\cos\theta_{km}) - V_k V_{cR}(g_{km}\sin(\theta_k - \theta_{cR}) - b_{km}\cos(\theta_k - \theta_{cR})) \quad (6)$$

$$P_{mk} = V_m^2 g_{mk} - V_k V_m (g_{km}\cos\theta_{mk} + b_{km}\sin\theta_{mk}) + V_m V_{cR}(g_{km}\cos(\theta_m - \theta_{cR}) + b_{km}\sin(\theta_m - \theta_{cR})) \quad (7)$$

$$Q_{km} = -V_m^2 b_{mm} - V_k V_m (g_{km}\sin\theta_{mk} - b_{km}\cos\theta_{mk}) + V_m V_{cR}(g_{km}\sin(\theta_m - \theta_{cR}) - b_{km}\cos(\theta_m - \theta_{cR})) \quad (8)$$

where

$$g_{km} + mb_{km} = 1/Z_{cR}, g_{kk} = g_{km}, b_{kk} = b_{km}$$

$$g_{mm} = g_{km}, b_{mm} = b_{km}$$

Operating constraint of the SSSC (active power exchange via the DC link) is as

$$PE = \mathrm{Re}(V_{cR} I^*_{mk}) = 0 \quad or$$

$$-V_k V_{cR}(g_{km}\cos(\theta_k - \theta_{cR}) - b_{km}\sin(\theta_k - \theta_{cR})) + V_m V_{cR}(g_{km}\cos(\theta_m - \theta_{cR}) - b_{km}\sin(\theta_m - \theta_{cR})) = 0 \quad (9)$$

The active power flow constraint is

$$P_{mk} - P_{mk}^{specified} = 0 \quad (10)$$

$$Q_{mk} - Q_{mk}^{specified} = 0 \quad (11)$$

Where

$P_{mk}^{specified}$ Is specified active power flow.

The equivalent voltage injection $V_{cR}\angle\theta_{cR}$ bound constraints are as

$$V_{cR}^{\min} \le V_{cR} \le V_{cR}^{\max} \quad (12)$$

$$\theta_{cR\min} \le \theta_{cR} \le \theta_{cR\max} \quad (13)$$

IV. STATIC SECURITY INDEX (SSI)

From the past decades, a rapid growth is evident with the usage of fuzzy logic applications. Reasoning modes can be applied effectively using fuzzy logic (FL). Instead numbers, the words are considered to define the mapping rule of fuzzy logic. Tolerance and impression are explored using the words computed by the FL. Furthermore, the output and input spaces can be mapped effectively using FL. Nonetheless, the multi-output and multi-input systems are modeled accurately using FL tool.

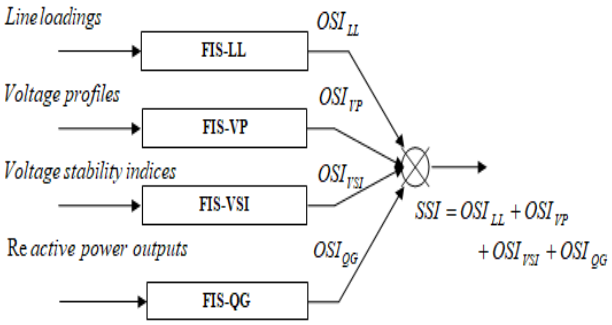

Figure 2: Parallel operated fuzzy inference systems

In the literature, different types of objective functions were used for optimization of power system operation. But, no one has evaluated the impact of the optimization of a particular objective function on the power system severity/security. Therefore, in order to evaluate the impact of optimization of power system operation, a fuzzy logic composite criteria based severity index is proposed in this case. Using this FL based static severity index, the impact on network contingency ranking is also evaluated.

FL based static security/severity index: As indicated in Fig 2, the parallel operated fuzzy inference systems (FIS) has adopted the severity index to obtain the total fuzzy logic composite criteria. For contingency, the static severity index is computed. When compared to the pre-fixed value, the severity index showing higher value is ranked after listing out [36].

V. OPF PROBLEM FORMULATION

Formulation of transient stability constrained standard OPF problem is as follows:

$$\text{Min} \quad f(\mathbf{u},\mathbf{x}) \tag{14}$$

$$\text{Subject to} \quad g(\mathbf{u},\mathbf{x}) = 0 \tag{15}$$

$$h(\mathbf{u},\mathbf{x}) \le 0 \tag{16}$$

Here, the control variables vector is indicated as $\mathbf{u}$ and the variable that corresponds to the dependent variable vector is indicated as $\mathbf{x}$, respectively.

Objective functions: Three different forms of objective functions included in the OPF problem are as follows:

Objective Function I :

$Min \quad f_1 = F_T = \sum \left(a_i P_{gi}^2 + b_i P_{gi} + c_i\right)$ is the cost of generation

Objective Function II :

$Min \quad f_2 = Ploss = \sum_{\substack{k\in N_l \\ k=(i,j)}} g_k (V_i^2 + V_j^2 - 2V_i V_j \cos\theta_{ij})$,

is the power loss

Objective Function III : $Min \quad f_3 = Lj2s = \sum_{j=g+1}^{nb} L_j^2$ is the sum of squared voltage stability indices

Constraints: The OPF problem constraints are categorized into two forms:

Equality Constraints: These constraints represent the sets of nonlinear equations for power flows, which means,

$$P_{Gi} - P_{Di} - \sum_{j=1}^{n} |V_i||V_j||Y_{ij}| \cos(\theta_{ij} - \delta_i + \delta_j) = 0 \tag{17}$$

$$Q_{Gi} - Q_{Di} + \sum_{j=1}^{n} |V_i||V_j||Y_{ij}| \sin(\theta_{ij} - \delta_i + \delta_j) = 0 \tag{18}$$

where P_{Gi} and Q_{Gi} are the real and reactive power outputs injected at bus i respectively, the load demand at the same bus is represented by P_{Di} and Q_{Di}, and elements of the bus admittance matrix are represented by $|Y_{ij}|$ and θ_{ij}.

Inequality Constraints: These constraints that represent the power system operational and security limits such as the bounds on the following:

Generators real and reactive power outputs

$$P_{Gi}^{\min} \le P_{Gi} \le P_{Gi}^{\max}, i = 1,\text{K}, N \tag{19}$$

$$Q_{Gi}^{\min} \le Q_{Gi} \le Q_{Gi}^{\max}, i = 1,\text{K}, N \tag{20}$$

Voltage magnitudes at each bus in the network

$$V_i^{\min} \le V_i \le V_i^{\max}, i = 1,\text{K}, NL \tag{21}$$

Transformer tap settings

$$T_i^{\min} \le T_i \le T_i^{\max}, i = 1,\text{K}, NT \tag{22}$$

Reactive power injections due to capacitor banks

$$Q_{Ci}^{\min} \le Q_{Ci} \le Q_{Ci}^{\max}, i = 1,\text{K}, CS \tag{23}$$

Transmission lines loading

$$S_i \le S_i^{\max}, i = 1,\text{K}, nl \tag{24}$$

Voltage stability index:

$$L_j \le L_j^{\max}, \qquad j = 1,\text{K}, NL \tag{25}$$

FACTS device constraint:

$V_{cR}^{\min} \le V_{cR} \le V_{cR}^{\max}$ SSSC voltage magnitude (26a)

$\theta_{cR}^{\min} \le \theta_{cR} \le \theta_{cR}^{\max}$ SSSC voltage angle (26b)

Transient stability constraint

$$|\delta_i - \delta_{COI}|_{max} \le \delta_{max} \qquad i = 1\ldots N_g, \tag{27}$$

A system maintaining stability followed with contingency 'k' is implied using the transient stability associated constraints as indicated in Equation (27). Power system ability is indicated using the term Transient stability index (TSI), which can be used to return back a new stable equilibrium by maintaining itself in its stable domain.

Transient stability constraints: Wide scopes of algebraic equations are used to explain the transient stability problem of power system. For the generator, the oscillation equations derived are as follows:

$$\dot{\delta}_i = w_i - w_0 \qquad i=1\ldots N_g \tag{28}$$

$$M_i \dot{\omega}_i = \omega_0 (P_{mi} - P_{ei} - D_i \omega_i) \tag{29}$$

Here, the synchronous speed is indicated as ω_o, for the i^{th} generator, the electrical output power is denoted as P_{ci}, mechanical input power as P_{mi}, damping constant as D_i, moment of inertia as M_i, rotor speed as ω_i, and rotor angle as δ_i, respectively.

Likely, the center of inertia (COI) position is expressed as follows:

$$\delta_{COI} = \frac{\sum_{i=1}^{N_g} M_i \delta_i}{\sum_{i=1}^{N_g} M_i}. \tag{30}$$

Equation (31) indicates the formulation of transient stability's inequality constraints.

$$|\delta_i - \delta_{COI}|_{max} \le \delta_{max} \qquad i = 1\ldots N_g, \tag{31}$$

For the i^{th} generator, the rotor angles maximum deviation from the COI is indicated as $|\delta_i - \delta_{COI}|_{max}$ and based on the experience the maximum value allowed by the rotor angle is denoted as δ_{max}. In this study, the trial and error method is used to determine the value of δ_{max}. Most of the past literal works have shown different values for each system.

Fitness value computation: To the fuel cost, the state variables violations are added to determine the fitness value of an individual. Normally, using Newton-Raphson algorithm, the fuel cost value is evaluated. Consequently, for each solution, the fitness value is evaluated as follows:

$$f(x,u) = f_i + K_Q \sum_{i=1}^{N_g}(Q_{gi} - Q_{gi}^{lim})^2 + K_V \sum_{i=1}^{N_{pq}}(V_i - Vilim)2 + Ksi{=}1Nl(Sl - Sllim)2$$

$$+ K_L \sum_{i=1}^{N_{pq}}(L_j - L_j^{lim})^2 + K_T \sum_{i=1}^{N_g}(|\delta_i - \delta_{COI}|_{max} - \delta^{lim})^2 . \quad (32)$$

Q_{gi}^{lim}, V_i^{lim}, S_i^{lim}, L_j^{lim}, and δ_i^{lim} are defined as follows:

$$Q_{gi}^{lim} = \begin{cases} Q_{gi}^{max};\ Q_{gi} > Q_{gi}^{max} \\ Q_{gi}^{min};\ Q_{gi} < Q_{gi}^{min} \end{cases} . \quad (33a)$$

$$V_i^{lim} = \begin{cases} V_i^{max};\ V_i > V_i^{max} \\ V_i^{min};\ V_i < V_i^{min} \end{cases} . \quad (33b)$$

$$L_j^{lim} = \begin{cases} L_j^{max};\ L_j > L_j^{max} \\ L_j^{min};\ L_j < L_j^{min} \end{cases} . \quad (34)$$

$$S_l^{lim} = \begin{cases} S_l^{max};\ S_l > S_l^{max} \\ S_l^{min};\ S_l < S_l^{min} \end{cases} . \quad (35)$$

$$\delta_i^{lim} = \begin{cases} \delta_{max};\ |\delta_i - \delta_{COI}|_{max} > \delta_{max} \\ 0:\ |\delta_i - \delta_{COI}|_{max} < \delta_{max} \end{cases} . \quad (36)$$

Here, the fitness function is indicated as $f(x,u)$. The transient stability limit, load bus voltage, the generator bus reactive power output, the slack bus reactive power output are indicated as K_T, K_L, K_s, K_V and K_Q, respectively. For the related variables, their upper or lower limits violations are indicated as Q_i^{lim}, V_i^{lim}, S_l^{lim} and L_j^{lim}, respectively. The number of load buses is indicated as N_{pq}, respectively. The penalty value is assumed to be zero when, the constraints relay within their lower and upper limits

VI. STANDARD DIFFERENTIAL EVOLUTION

Population initialization is the first step of DE algorithm. Initial population is formed through random generation of NP solutions group included in the control parametric space. Update of population from one cycle to the next cycle is performed soon after completing the initialization step. When reached maximum number of cycles, the repetition of process is stopped; otherwise, the process is continued until the termination criterion is attained. However, the mutation, crossover, and selection are the three kinds of operations used for updating the populations at each cycle or generations. Both crossover and mutation operations are applied to generate new solutions in every generation/iteration. Then, the appropriate solutions from these generated new solutions are obtained through applying the selection operation [37].

Individuals are referred to be the NP populations that are evolved using DE algorithm. In D-dimensional parametric space, the candidate solutions are encoded to achieve the global optimum (i.e. $X_{i,G} = \{X_{i,G}^1, \ldots\ldots, X_{i,G}^D\}, i = 1, \ldots\ldots, NP$). Inside the search space, the individuals are randomized uniformly considering the maximum and minimum parametric limits $X_{min} = \{X_{min}^1, \ldots\ldots, X_{min}^D\}$ and $X_{max} = \{X_{max}^1, \ldots\ldots, X_{max}^D\}$, respectively. For instance, at generation G=0, the ith individual containing the initial value of jth parameter is as follows:

$$x_{i,0}^j = x_{min}^j + rand(0,1) \cdot (x_{max}^j - x_{min}^j), \quad j = 1,2,3, \ldots\ldots, D \quad (37)$$

Here, the limit [0, 1] considered for uniform distribution of random variables is indicated as $rand(0,1)$.

Mutation Operation: Considering each individual $X_{i,G}$ (target vector) in the current population, the mutant vector $V_{i,G}$ is generated using the mutation operation applied by the DE algorithm after completing the initialization of population or solutions. From the below given mutation strategies, any one of them can be selected to generate the mutant vector $V_{i,G} = \{v_{i,G}^1, v_{i,G}^2, \ldots\ldots, v_{i,G}^D\}$ corresponding to each target vector $X_{i,G}$ at each cycle. In DE algorithm, the commonly used mutation operation strategies are provided below:

"DE/rand/1"

$$V_{i,G} = X_{r_1^i,G} + F \cdot \left(X_{r_2^i,G} - X_{r_3^i,G}\right) \quad (38)$$

"DE/best/1":

$$V_{i,G} = X_{best,G} + F \cdot \left(X_{r_1^i,G} - X_{r_2^i,G}\right) \quad (39)$$

"DE/rand − to − best/1": $V_{i,G} = X_{i,G} + F \cdot \left(X_{best,G} - X_{i,G}\right) + F \cdot \left(X_{r_1^i,G} - X_{r_2^i,G}\right)$ (40)

4) *"DE/best/2":*

$$V_{i,G} = X_{best,G} + F \cdot \left(X_{r_1^i,G} - X_{r_2^i,G}\right) + F \cdot \left(X_{r_3^i,G} - X_{r_4^i,G}\right) \quad (41)$$

5) "DE/rand/2":

$$V_{i,G} = X_{r_1^i,G} + F \cdot \left(X_{r_2^i,G} - X_{r_3^i,G}\right) + F \cdot \left(X_{r_4^i,G} - X_{r_5^i,G}\right) \quad (42)$$

Here, the indices generated are represented as $r_1^i, r_2^i, r_3^i, r_4^i,$ and r_5^i, respectively. They are called exclusive integers generated in mutual and random manner. For each mutant vector, the random generation of these indices is performed. Vector difference is scaled using a positive control and scaling factor denoted as F. In a specific generation, the best fitness value containing individual vector is represented as $X_{best,G}$.

Crossover Operation: A trial vector $U_{i,G} = (u_{i,G}^1, u_{i,G}^2, \ldots\ldots, u_{i,G}^D)$ is generated from the mutant vector $V_{i,G}$ and its relative target vector $X_{i,G}$ by means of applying the crossover operation. This process is done after finishing the mutation operation. Uniform (binomial) crossover employed for the basic DE algorithm is as follows:

$$u_{i,G}^j = \begin{cases} v_{i,G}^j, & if\left(rand_j[0,1) \le CR\right) or\ (j = j_{rand}) \\ x_{i,G}^j, & otherwise \end{cases} j = 1,2,\ldots\ldots,D. \quad (43)$$

Usually, the mutant vector is observed to copy the fraction of parameter values. These values are then controlled using a significant constant called crossover rate CR relaying in the limit [0,1] (as indicated in (43).

In case, if $rand_j[0,1) \leq CR$ or$j = j_{rand}$ then to the trial vector element $U_{i,G}$, the mutant vectors $V_{i,G}$ jth parameter is copied by the binomial crossover operator. If this is not the case, then the corresponding target vector $X_{i,G}$ is considered to copy the jth mutant vector parameter. Also, considering the target vector $X_{i,G}$, the trial vectors $U_{i,G}$ residual parameters are copied. Condition j_{rand} ensures that the trial vector $U_{i,G}$ will be different from its corresponding target vector $X_{i,G}$ by at least one parameter.

Selection Operation: Best population is obtained after employing the selection operation. Target vector $f(X_{i,G})$ is used to compare each trial vector $f(U_{i,G})$ and its relative objective function value. Compared to the target vector, the equal or less objective function value obtained by the trial vector can take place in the next cycle as an individual by replacing the target vector. If this is not the case then, the next cycle is continued with the target vector. Equation (44) indicates the selection operation.

$$X_{i,G+1} = \begin{cases} U_{i,G}, & if f(U_{i,G}) \leq f(X_{i,G}) \\ X_{i,G}, & otherwise \end{cases} \quad (44)$$

After reaching the termination criterion, the repetition of the process is stopped.

VII. ADAPTIVE UNIFIED DIFFERENTIAL EVOLUTION

Standard differential evolution algorithm has been improved using the newly proposed ten various forms of mutation strategies. When quantified numerous test samples of different optimization problems, the "DE/best /1/bin" has achieved good performance compared to "DE/ rand/1 bin". However, the ICEC96 contest has suggested using the DE/best /2/bin due to its excellent performance [38, 39]. Usage of differential evolution algorithm can cause difficulties with the existence of multiple mutation strategies. Works in [40-42] have proposed the techniques of combining different forms of multiple mutation strategies.

In this work, the differential evolution algorithm using many of the traditional mutation strategies are unified through developing a new single mutation expression. This can be expressed as follows:

$$v_i = x_i + F_1(x_b - x_i) + F_2(x_{r1} - x_i) + F_3(x_{r2} - x_{r3}) + F_4(x_{r4} - x_{r5}) \quad (45)$$

In the current iteration (generation), the best solution identified is indicated in the right side of Eq. (45) (i.e. in second term). From the random solution, the rational invariant contributions obtained are indicated in third term [43]. As similar to the normal differential evolution algorithm, the parent solutions differences are indicated in the 4th and 5th terms.

From the best solution, the mutated solutions are diverted away using the final three terms. This helps in the improvement of exploration process of the algorithm during making decision in the parametric space. The weights obtained are represented using four parameters such as, F_1, F_2, F_3 and F_4. In order to produce a new mutant solution, the exploration and exploitation are combined using mutation expression operation. Mutation operators space is explored widely using an opportunity provided by this new expression.

It is possible to achieve a new mutation strategy during applying a differential set of parameters such as, F_1, F_2, F_3, and F_4. Compared to the most of the traditional standard differential evolution algorithms, a better optimization solution can be obtained using a unified mutation strategy.

During performing different optimization stages, various combinations of mutation strategies can be applied through adjusting the differential set of parameters at each evolution of the optimization process. Hence, the simplicity in mathematical expressions is enjoyed in these unified mutation operations.

Different mutation strategies are used and combined using a method provided by the unified mutation strategy. Thereby, the application users have considered the selection of suitable control parameters F_1, F_2, F_3, and F_4 is a time consuming and tedious process. Performance of the algorithm is highly improved and the computational burden of the application users is reduced on selecting the control parameters using a self-adaptive method.

In past studies, a number of parameters control methods were used for the conventional differential evolution algorithm [44-48]. The proposed unified differential algorithm in this work is developed through evolving dynamically the five control parameters F_1, F_2, F_3, F_4 and C_r of classical self-adaptive method. In most of the experimental tests, the good performance was achieved using this simple self-adaptive scheme.

In this study, a set of control parameters $x_i, i = 1,2,3,....NP$ are comprised in each individual solution during the generation G of the mutation process in self-adaptive method. A new control parameter sets $F_{1,i}^{G+1}, F_{2,i}^{G+1}, F_{3,i}^{G+1}, F_{4,i}^{G+1} and C_{r_i}^{G+1}$ are computed prior to the adaptation of unified differential evolution expressions for producing a new mutant solution.

$$F_{j,i}^{G+1} = \begin{cases} F_{jmin} + r_{j1}(F_{jmax} - F_{min}), & if r_{j2} < \tau_j \\ F_{1,iotherwise}^{G} \end{cases} \quad (46)$$

$$C_{r_i}^{G+1} = \begin{cases} C_{r_{min}} + r_3(C_{r_{max}} - C_{r_{min}}), & if r_4 < \tau_5 \\ C_{r_{i,}}^{G} & otherwise \end{cases} \quad (47)$$

Maximum and minimum values of the control parameters are expressed as $F_{jmin} and F_{jmax}$ for j=1, 2, 3, 4; whereas, the uniform random values distributed in the interval [0,1] are indicated as r_{j1}, r_{j2}, $j = 1,2,3$, r_3, r_4 , respectively. Subsequently, the maximum and minimum cross over probability of the control parameters are denoted as $C_{r_{max}}$ and $C_{r_{min}}$. For the j^{th} control parameter, the probability of old value and new value used is indicated as τ_j, j=1, 2,3,4,5. Notably, it is important to maintain the value of τ_j to be smaller for further generating the new trial solutions by means of reusing the survived solutions. In this work, the value of τ_j is fixed to 0.1. Also, the values 0 and 1 are fixed to $F_{jmin} and F_{jmax}$, respectively. The control parameters values are fixed to $C_{r_{max}}$=1 and $C_{r_{min}}$ =0. Based on different traditional mutation strategies, the values for these parameters are selected.

However, the mutant solution is generated using this new control parameter step. In between the minimum and maximum values, the initial values for the control parameters are assigned. Pseudo-code of the AuDE algorithm is indicated below as follows:

Pseudo-code of AuDE algorithm: Based on uniform samplings distributed randomly in the interval [0,1], the initial control parameters F_1, F_2, F_3, F_4, C_r are generated. The NP points are sampled randomly inside the feasible control parametric space x to generate a set of initial population. Then, their corresponding objective function values f(x) are evaluated.

Initialize the generation number as G=0
While not attained the stopping criteria, Do:
For i=1to NP (for each parent solutions target x_i):
Mutation
Determine a set of control parameters (for j=1, 2, 3, and 4):

$$F_{j,i}^{G+1} = \begin{cases} F_{jmin} + r_{j1}(F_{jmax} - F_{min}), & if r_{j2} < \tau_j \\ F_{1,iotherwise}^{G} \end{cases}$$

$$C_{r_i}^{G+1} = \begin{cases} C_{r_{min}} + r_3(C_{r_{max}} - C_{r_{min}}), & if r_4 < \tau_5 \\ C_{r_{i,}}^{G} & otherwise \end{cases}$$

Using AuDE mutation strategy to determine a mutant solution vector:

$$v_i = x_i + F_1^{G+1}(x_b - x_i) + F_2^{G+1}(x_{r1} - x_i) + F_3^{G+1}(x_{r2} - x_{r3}) + F_4^{G+1}(x_{r4} - x_{r5})$$

Crossover
Generate a new trial solution $U_i(u_{i1}, u_{i2}, \ldots\ldots\ \ldots, u_{iD})$ through binomial crossover scheme:
u_{ij}=u_{ij} if $rand_{ij}[0,1] \leq C_{r_i}^{G+1}$ or j=$j_{rand,}$
Otherwise $u_{ij} = x_{ij}$
Selection
For the trial solution $f(U_i)$ compute the objective functions
If $f(U_i) \leq f(x_i)$ then $x_{i,G+1} = U_i$
Else $x_{i,G+1} = x_{i,G}$
Find For
G=G+1
End While

VIII. IMPLEMENTATION OF AUDE ALGORITHM FOR OPF PROBLEM

Number of populations (N_p) is significantly adopted by the natural evolution algorithm called differential evolution to attain an optimal solution through repeating the iterations. In this section, the adaptive unified differential evolution algorithm is applied to solve TSCOPF problem. Initialization, selection, and evaluation of solutions are the three most important strategies introduced by the differential evolution algorithm (DEA). However, these strategies mainly aimed for the minimization of computational time. The flow chart of the proposed AuDE algorithm for solving the TSCOPF problem is illustrated in Fig.3. Detailed explanation is provided in this section.

Using individuals (populations) to encode the control variables: In order to withstand the TSCOPF issues, the differential algorithm should be applied only after identifying the number of control variables from the problem that are need to be optimized. Here, Q_{ci} indicates the shunt reactive power, T_{ti} as tap changing transformers, V_{gi} as voltage magnitudes generator, and P_{g1} is the slack unit not considered in P_{gi} known as the outputs of the active power generator. Therefore, u can be expressed as

$$u^T = [P_{g2}, \ldots\ldots P_{gNg}, V_{g1}, \ldots\ldots V_{gNg}, T_{t1}, \ldots\ldots T_{tNt}, Q_{C1}, \ldots\ldots Q_{CNc}] \quad (48)$$

Selecting the size of population:- Problem size is adopted for accurate selection of the population size (N_p). Considering C as the control variables in most of the real world engineering problems, then obtaining optimal solutions with $N_p < 2C$ is a complex process and easier with $N_p = 20C$ condition [49]. Furthermore, the possible optimal solutions are obtained using the population size $N_p = 3-5C$

In AuDE algorithm, the populations are initialized through employing the OBL scheme. This process is done to improve the solution quality [50].

Based on Eq. (49), an individual u containing the control variables are generated randomly within a specific limit. However, the first iteration has used these randomly generated individuals as the root (parent) population.

$$u_{i,j}^0 = rand(0,1) * \left(u_j^{max} - u_j^{min}\right) + u_j^{min} \quad (49)$$

$$ou_{i,j}^0 = u_j^{\min} + u_j^{\max} - u_{i,j} \text{ //opposition-based learning}$$

Selecting N_P fittest individuals from set the $\{u_{i,j}^0, ou_{i,j}^0\}$ as initial population;

At the k^{th} generation, the control variables j in a population i is indicated as $u_{i,j}^k$ representing $i \in \{1,2,3,\ldots.,N_p\}$ and $j \in \{1,2,3,\ldots.,N_p\}$, respectively. For the control variable j, their upper and lower limits are indicated as $u_j^{\min}$ and $u_j^{\max}$.

Below said procedures are followed for satisfying the constraints in slack bust active power. Consider P_L as the total active load of the system, P_{ds} be the power summed through not including the slack unit as well as dispatching from all the generators. Subsequently, the slack bus generator active power is assigned with a value obtained by means of subtracting P_{ds} from P_L. In case, if the slack bus generators upper or lower limits are exceeded by the value assigned to the slack bus active power, then the limits P_{slack}^{max} or P_{slack}^{min} are fixed to its active power. The other generators are assigned with the residual active power, proportionally.

Implementing load flow technique: In order to compute the power flow solutions, the Newton-Raphson power flow program is implemented for each population (individual). Indices of voltage stability, line flows, load bus voltages, outputs of the reactive power are considered as the constraints of power system operation.

These constraints are verified and the slack bus (independent generator) generations are calculated during evaluating the power flow solutions.

Fitness Computation: Each individual's quality can be measured by evaluating every individual solution using penalty functions included in the fitness measure F_i as shown below:

$$F_i = 1/(f_i + K_Q F_{Qi} + K_v F_{Vi} + K_S F_{Si} + K_L F_{Li} + K_T F_{Ti}) \quad (50)$$

$$F_{Qi} = \sum_{l=1}^{N_g} (|Q_{Gil} - Q_{Gil}^{lim}|)^2 \quad (51a)$$

$$F_{Vi} = \sum_{l=1}^{N_{pq}} (|V_{il} - V_{il}^{lim}|)^2 \quad (51b)$$

$$F_{Si} = \sum_{l=1}^{Nl} (|S_{li} - S_{li}^{lim}|)^2 \quad (53a)$$

$$F_{Li} = \sum_{l=1}^{Npq} (|L_j - L_j^{lim}|)^2 \quad (53b)$$

$$F_{Ti} = \sum_{i=1}^{N_g} (|\delta_i - \delta_{COI}|_{max} - \delta^{lim})^2 \quad (54)$$

Here, the fuel costs (f_i) generated by the system is represented as F_{Qi}, F_{Vi}, F_{Si}, F_{Li} and F_{Ti}, respectively. For each individual i, the outputs of reactive power generators corresponding normalized violations summations, rotor angles generator, voltage stability indices, and PQ-bus voltages are also shown in Eq. (54)

N_{pq} is the total number of PQ buses, N_g is the total number of generator, N_l is the total number of lines; Q_{gil}^{lim}, V_{il}^{lim}, S_{il}^{lim}, L_{jil}^{lim} and δ^{lim} denote the violated upper and lower limits of the generator reactive power outputs, voltages of the load buses, line flows, voltage stability indices of load buses and generator rotor angle respectively; K_Q, $K_v K_S K_L$ and K_T are the corresponding penalty coefficients. Ultimately, if obtained higher the fitness value, then better the individual is generated.

Assessment of transient stability: Actually, the TSCOPF optimization problems have large searching space; thereby, it is a time-consuming process to assess the transient stability constraints. Hence, during TSA computation process, the populations (individuals) with good fitness alone are allowed to determine the stable and feasible optimal solutions. This process has reduced the computational burden by not delimiting the evolutions reproduction abilities. By the fact, the fitness function has included in the transient stability to satisfy its conditions neither for satisfying the optimization objectives. Therefore, before going to the evaluation of transient stability, each individual is evaluated for the SSI values whose value is less than or equal to the specified value. During evolution, the selection process will be maintained effectively through handling the system stability in a chosen contingency using that specific individual.

Global best individual: From all generations, the best individual obtained is indicated as u_{best}(i.e. the global best individual). To find u_{best} individuals, two individuals u_a and u_b are compared in a particular generation, u_a is defined" better" than u_b if matched any one of the below given criterions:

Higher fitness value is for u_a and both of them are stable

Higher fitness value is for u_a and both of them are unstable

Instability is for u_b and stability for u_a

Mutation operation: Different evolution algorithms that have used few traditional mutation strategies are unified with the aid of a single mutation expression. This is expressed as follows:

$$v_i = x_i + F_1^{G+1}(x_b - x_i) + F_2^{G+1}(x_{r1} - x_i) + F_3^{G+1}(x_{r2} - x_{r3}) + F_4^{G+1}(x_{r4} - x_{r5}) \quad (55)$$

In order to produce a new mutant solution, the exploration and exploitation are combined using mutation expression operation. Mutation operators space is explored widely using an opportunity provided by this new expression. It is possible to achieve a new mutation strategy during applying a differential set of parameters such as, F_1, F_2, F_3, and F_4. Compared to the most of the traditional standard differential evolution algorithms, a better optimization solution can be obtained using a unified mutation strategy.

At the time of performing different optimization stages, various combinations of mutation strategies can be applied through adjusting the differential set parameters during each evolution of the optimization process. Hence, the simplicity in mathematical expressions is enjoyed in these unified mutation operations. The proposed unified differential algorithm in this work is developed through evolving dynamically the five control parameters F_1, F_2, F_3, F_4 and C_r of classical self-adaptive method. In most of the experimental tests, the good performance was achieved using this simple self-adaptive scheme.

In this study, a set of control parameters $x_i, i = 1,2,3,....NP$ are comprised in each individual solution during the generation G of the mutation process in self-adaptive method. A new control parameter sets $F_{1,i}^{G+1}, F_{2,i}^{G+1}, F_{3,i}^{G+1}, F_{4,i}^{G+1} and C_{r_i}^{G+1}$ are computed prior to the adaptation of unified differential evolution expressions for producing a new mutant solution.

$$F_{j,i}^{G+1} = \begin{cases} F_{jmin} + r_{j1}(F_{jmax} - F_{min}), & if r_{j2} < \tau_j \\ F_{1,i otherwise}^{G} \end{cases} \quad (56)$$

$$C_{r_i}^{G+1} = \begin{cases} C_{r_{min}} + r_3(C_{r_{max}} - C_{r_{min}}), & if r_4 < \tau_5 \\ C_{r_{i,}}^{G} & otherwise \end{cases} \quad (57)$$

Maximum and minimum values of the control parameters are expressed as $F_{jmin} and F_{jmax}$ for j=1, 2, 3, 4; whereas, the uniform random values distributed in the interval [0,1] are indicated as r_{j1}, r_{j2}, $j = 1,2,3$, r_3, r_4, respectively. Subsequently, the maximum and minimum cross over probability of the control parameters are denoted as $C_{r_{max}}$ and $C_{r_{min}}$. For the j^{th} control parameter, the probability of old value and new value used is indicated as τ_j, j=1, 2,3,4,5. Notably, it is important to maintain the value of τ_j to be smaller for further generating the new trial solutions by means of reusing the survived solutions.

Crossover Operation: A trial vector $U_{i,G} = (u_{i,G}^1, u_{i,G}^2, \ldots, u_{i,G}^D)$ is generated after performing the mutation operation. In other words, this trial vector is generated through applying crossover operation to the mutant vector $V_{i,G}$ and to its target vector pairs $X_{i,G}$. Uniform (binomial) crossover is employed to the AuDE as follows:

$$u_{i,G}^j = \begin{cases} v_{i,G}^j, & if\left(rand_j[0,1) \le CR\right) or\ (j = j_{rand}) \\ x_{i,G}^j, & otherwise \end{cases} \quad j = 1,2,\ldots,D. \qquad (58)$$

In case, if $rand_j[0,1) \le CR$ or $j = j_{rand}$ then to the trial vector element $U_{i,G}$, the mutant vectors $V_{i,G}$ jth parameter is copied by the binomial crossover operator. If this is not the case, then the corresponding target vector $X_{i,G}$ is considered to copy the j[th] mutant vector parameter. Also, considering the target vector $X_{i,G}$, the trial vectors $U_{i,G}$ residual parameters are copied. Condition j_{rand} ensures that the trial vector $U_{i,G}$ will be different from its corresponding target vector $X_{i,G}$ by at least one parameter.

Verifying the boundary limits: During evaluating the evolutionary based optimization algorithms, their unavoidable constraints are handled in numerous ways. In case, if any of the individual element in the AUDE algorithm drops its corresponding inequality constraints, then the minimum/maximum operating point is fixed based on the individual position.

Analysis of power flow to offspring individuals: Each offspring individuals power flow solutions are computed using a Newton-Raphson power flow program. The slack bus generators corresponding generations are calculated during this process. Then, the fitness function is evaluated through verifying the constraints of power system operation (voltage stability indices, line flows, load bus voltages, and reactive power outputs).

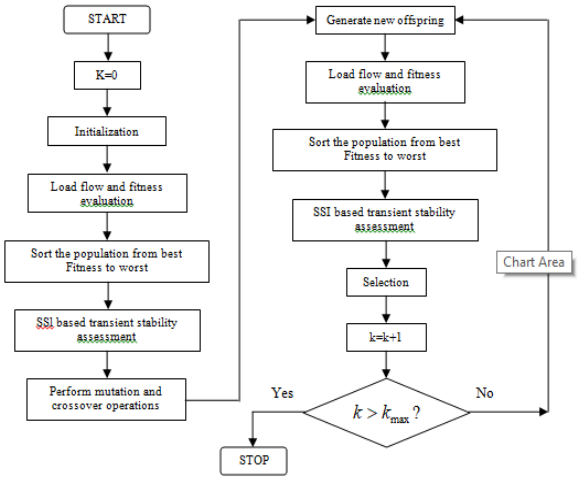

Figure 3: Flow chart for solution of TS-OPF problem

Transient stability assessment: By the fact, the fitness function has included in the transient stability to satisfy its conditions neither for satisfying the optimization objectives. Therefore, before going to the evaluation of transient stability, each individual is evaluated for the SSI values whose value is less than or equal to the specified value. During evolution, the selection process will be maintained effectively through handling the system stability in a chosen contingency using that specific individual.

Selection: A "one- to-one" selection process actually indicates this selection scheme. Ultimately, the best individual is selected by comparing the parent individual u_i^k to its offspring individual $u^{'k}$. In the next generation, the parent population was obtained from the previous updated population of generation 'k' (i.e. the selected individuals).

Updating the global best individual: From the generation k, the updated population's best individuals are determined and denoted as u_{best}^k. When compared to u_{best}, if found the better one is u_{best}^k then, using u_{best}^k the term u_{best} is replaced.

Verifying end condition: The iteration process is repeated continuously until the end condition is attained. In this work, after satisfying the given criterion, the iteration of AuDE is stopped: At any time a pre-determined generations are achieved, then it is possible to stop the optimization process.

IX. SIMULATION RESULTS

The IEEE test systems such as, 39-bus, New England ten-generator, and 30-bus, six-generator systems are used to test the effectiveness of proposed AuDE method. Constant impedance models of the loads and synchronous generators are modeled using the traditional generator model. Here, the simulation period is fixed to 2.0s and transient stability simulation is performed using 0.01s as integration time step. Reliability and robustness of the proposed AuDE method is verified through performing 20 trial runs for each test case. Implementation is done using MATLAB 7.8 software. The hardware components adopted for implementation are 2.0GB RAM PC, and Intel Core 2 Duo of 2 GHz.

A. Results of IEEE 30-bus system

The 30-bus test system consists of a transmission network of 41 branches with interconnection of six generating units as shown in Fig. 4. However, the total real and reactive power loads in the transmission network is 283.4 MW and 126.2 MVAR respectively. Ref. [51] is used to obtain the branch and bus data. Here, off-nominal tap ratio is included in 4 transformers. For buses 10, 12, 15, 17, 20, 21, 23, 24 and 29, the shunt injections are applied. In this work, the swing bus is assumed to be bus 1. Also, it is used to consider the real power generations with its minimum and maximum limits, and cost coefficients [51]. The value 0.9 and 1.1 pu is fixed to be the minimum and maximum limits of the control variables of tap changing transformer. Conversely, the value 0.9 and 1.1 pu is fixed to be the minimum and maximum limits of voltages of generators. For load buses, their minimum and maximum voltages used are 0.95 and 1.1, respectively. Ref [52] is used to fix the limits of line flows.

In the simulation studies of Case 1, a fuzzy logic based SSI for network contingency ranking is carried out to determine the rank-1 network contingency. The FL based network contingency method takes the pre/post contingency line loadings, load bus voltages, voltage stability indices, and reactive power outputs of generators for ranking. Instead of assessing the transient stability under the randomly selected network contingency,

the TSA is done under the rank-1 network contingency for testing the effectiveness of the proposed algorithm. In Case 2 simulation studies, the proposed AuDE method is applied for solving the transient stability constrained optimal power flow problem without and with SSSC device under the rank-1 network contingency condition. Various equality and inequality constraints, including the voltage stability and transient stability constraints are considered during the solution of the TS-OPF problem.

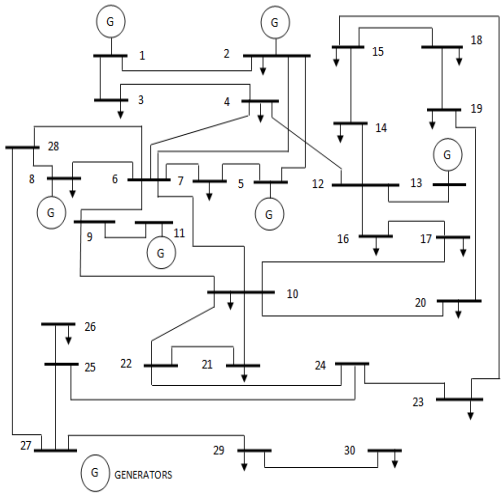

Figure 4: IEEE 30-bus test system indicated using single line diagram

Case 1: Fuzzy approach for contingency ranking: Network contingencies are ranked by means of applying the proposed FL based SSI approach. Thereby, the most threatening contingencies are identified from the base-load conditions and base-case control variables. Given input values are taken into account by the parallel operated fuzzy inference systems to find the network contingency and its total fuzzy logic based SSI (Fig. 2). Work in [36] has detailed the FL based SSI approach. Tables 1 and 2 provided the contingency analysis results. The line outages that results in heavy overload conditions are the line outages 8-11, 27-30, 27-29, 9-10, and 10-20. On the other hand, Table 1 has shown ranking of top 5 contingencies. Moreover, the table also depicts the outcomes of top 5 network contingencies namely, outputs of generator reactive power, voltage stability indices, voltage profiles, and line loading of severity indices. For network contingencies, different forms of severity indices (number of load buses, number of lines) determined are illustrated in Table 2. Highest total severity index (i.e. the most severe line outage 8-11) can be observed from both the Tables 1 and 2.

Case 2: TSOPF with SSSC device: In this Case 2, the transient stability constrained optimal power flow issues are solved using the proposed algorithm, which was tested through minimizing the number of objective functions. Sum of squared voltage stability indices, real power loss, and quadratic fuel cost function are considered as the objective functions. All the constraints such as, voltage stability, inequality, and equality, are augmented with objective functions is performed. The proposed AuDE algorithm is applied with SSSC device to solve the transient stability constrained optimal power flow issues in the presence of SSSC. The SSSC device is located in the line connected between buses 17 and 12 which is carrying the lowest line flows with base case operation.

The value 150 is fixed as the required number of iterations/generations and the size of population is fixed to 50. For TSA, the individual population whose SSI value is less than the specified value is considered for the transient stability assessment under the rank-1 contingency case which is obtained in the previous section. A large disturbance is created by tripping line 8-11. Line flow limits and reactive power generation limit constraints satisfaction is achieved by these solutions.

Figs.5-7 shows the convergence of the cost of generation, power loss and sum of squared voltage stability indices with the AuDE algorithm for the best run with SSSC device. From the Figs.5-7 it can be observed that the AuDE algorithm reaches the best solution within 100 iterations with SSSC during minimization of cost objective function. Also, it can be observed that during the iterative process, the proposed AuDE algorithm converges to global solution within 150 iterations of the algorithm during minimization of power loss and voltage stability index.

The optimal settings of the control variables for the best result of OPF problem obtained by the AuDE method without and with SSSC are given in Table 3 respectively. The cost of generation, real power loss, maximum voltage stability index, and computation time are also given in Table 3. It can be found that the proposed AuDE method gives lower values for cost of generation, power loss and voltage stability index than the values obtained without the SSSC device. Also the cost of generation, power loss and voltage stability index are decreased with the SSSC and transient stability constraints.

The Figs. 8-10 show the stable trajectories of relative rotor angles of best solutions obtained with AuDE algorithm with SSSC device. The load bus voltages, voltage stability indices and percentage line loadings with SSSC device are maintained within their lower and upper limits after optimization with SSSC device and are shown Figs.11-13 respectively. The comparison of the cost of generation for base case OPF with other methods reported in the literature is given in Table 4. It can be seen from the Table 4 that the proposed AuDE algorithm gives best cost of generation for base case OPF (neglecting voltage/transient stability constraints) compared with other methods reported in the literature.

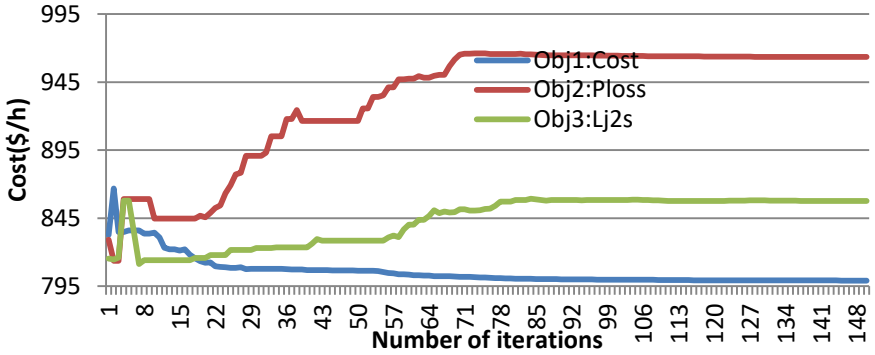

Figure 5:Convergence of cost of generation of IEEE 30-bus during optimization of different objective functions

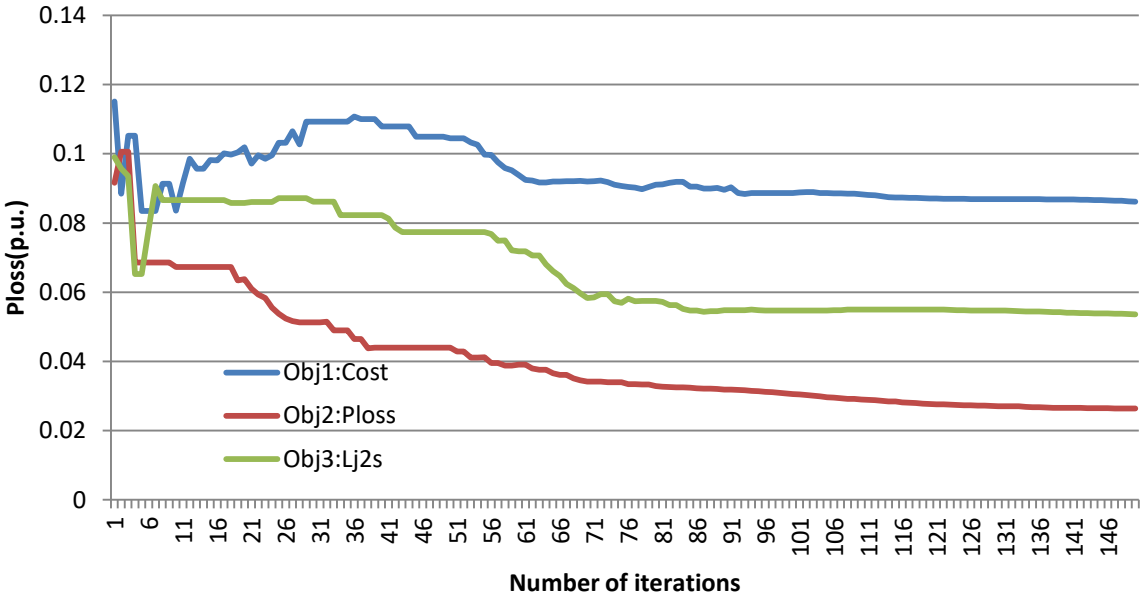

Figure 6: Convergence of real power loss of IEEE 30-bus during optimization of different objective functions

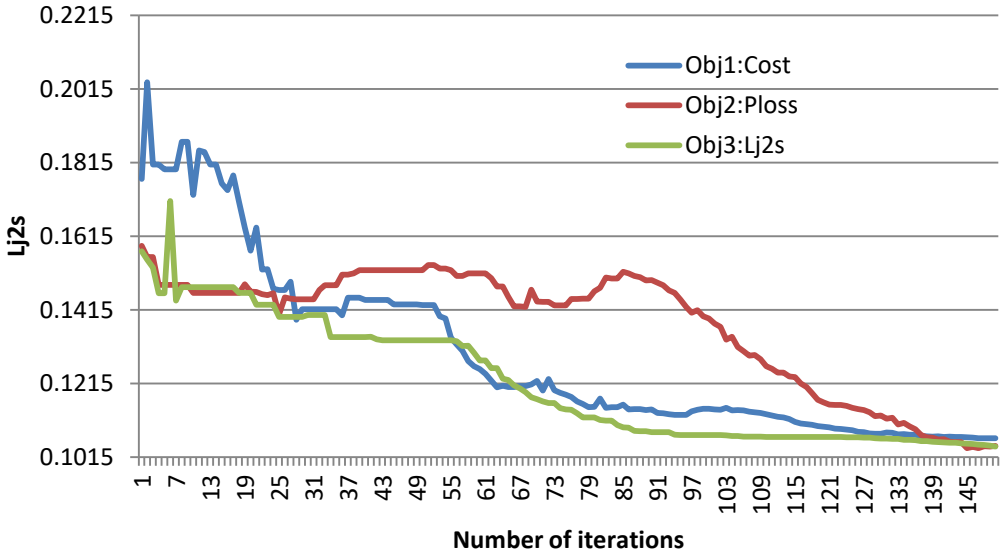

Figure 7: Convergence of sum of squared voltage stability indices of IEEE 30-bus during optimization of different objective functions

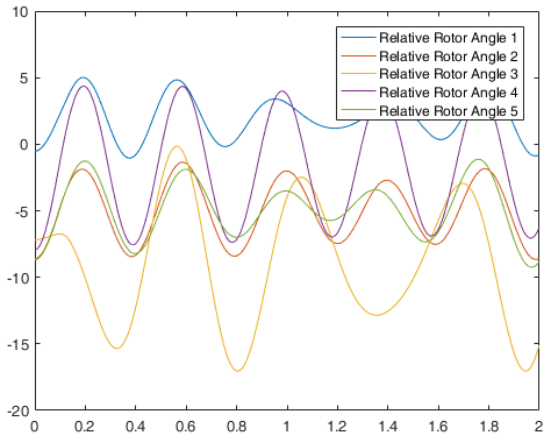

Figure 8: Stable trajectories of rotor angles of IEEE 30-bus with fuel cost optimization

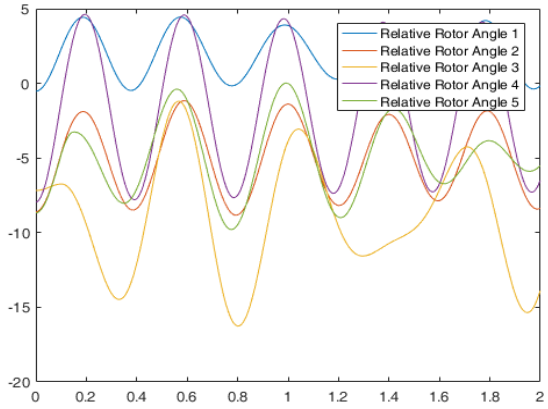

Figure 9: Stable trajectories of rotor angles of IEEE 30-bus for real power loss optimization

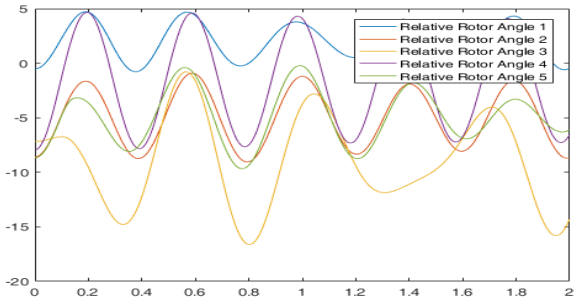

Figure 10: Stable trajectories of rotor angles of IEEE 30-bus for voltage stability optimization

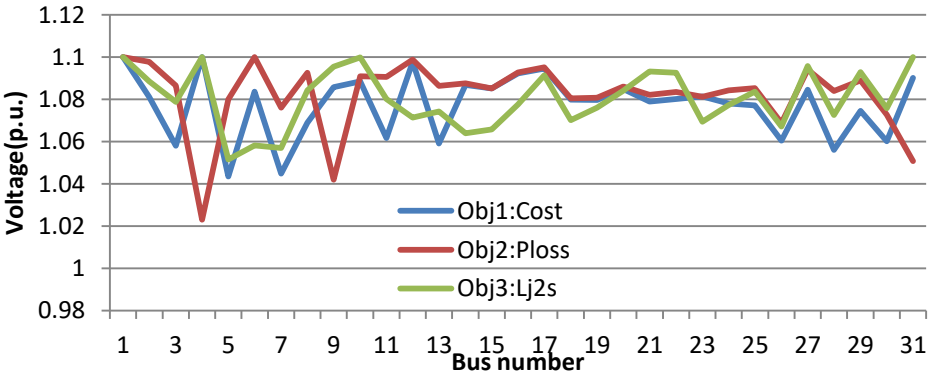

Figure 11: Voltage profiles of IEEE 30-bus system after optimization of different objective functions

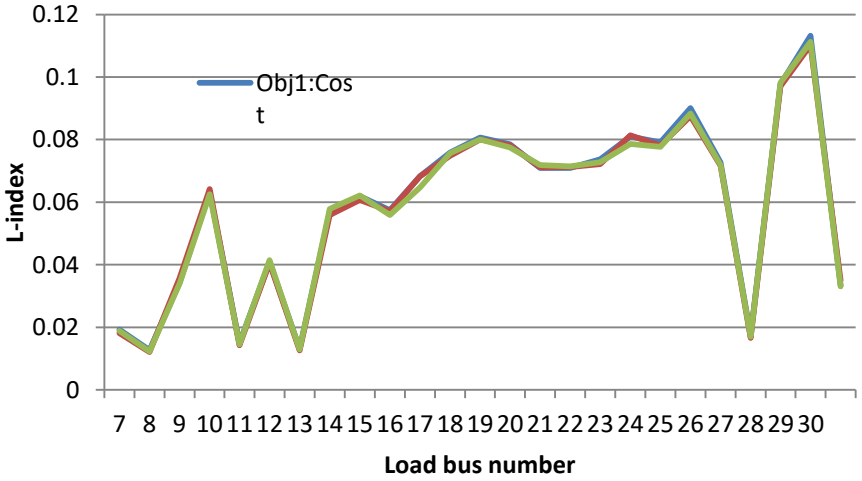

Figure 12: Voltage stability indices IEEE 30-bus system after optimization of different objective functions

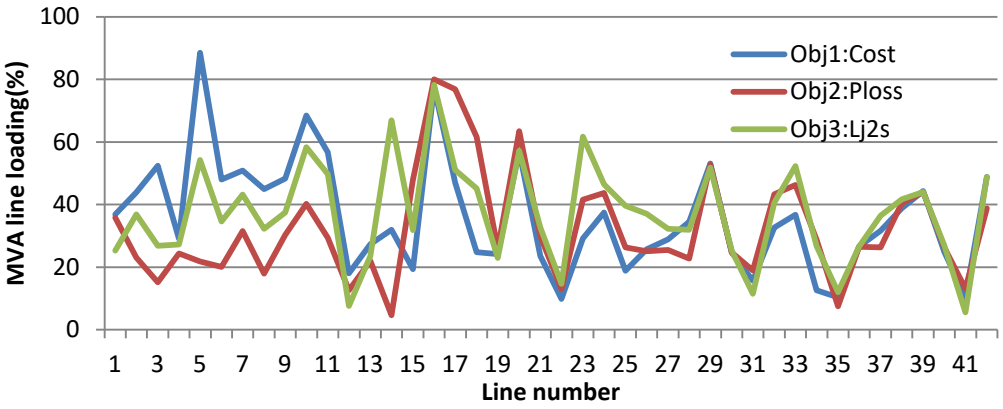

Figure 13: Percentage line loadings of IEEE 30-bus system after optimization of different objective functions

Table 1 Contingency Ranking of IEEE 30-bus system

Contingency	OSI_{LL}	OSI_{VP}	OSI_{VSI}	OSI_{QG}	FLCC	Ploss(p.u.)	Ljmax	Rank
8-11	362.5	306.9996	96.0019	144.9996	910.5011	0.0718	0.1473	1
27-30	393.75	306.9996	108.0018	54	862.7515	0.0586	0.2389	2
27-29	375	302.9649	120.0017	54	851.9666	0.0573	0.2719	3
9-10	456.25	216	96.0019	54	822.2519	0.0586	0.1681	4
10-20	456.2496	216	96.0019	54	822.2515	0..582	0.1562	5

Table 2 Number of lines/buses under different severity category before optimization

Contingency	Line Loading				Voltage Profile			Voltage Stability Indices					Reactive power outputs			Rank
	LS	BS	AS	MS	BS	AS	MS	VLS	LS	BS	AS	MS	BS	AS	MS	
8-11	34	6	0	0	23	0	1	24	0	0	0	0	5	0	1	1
27-30	34	5	1	0	23	0	1	23	1	0	0	0	6	0	0	2
27-29	35	4	1	0	23	0	1	22	2	0	0	0	6	0	0	3
9-10	29	11	0	0	24	0	0	24	0	0	0	0	6	0	0	4
10-20	33	6	0	1	24	0	0	24	0	0	0	0	6	0	0	5

Table 3 Optimal setting of control variables for IEEE 30-bus system with SSSC

Control variables(p.u.)	Base Case	OPF (without SSSC	Objective functions		
			Cost	PLoss	Lj2s
	0.9873	1.7730	1.7732	0.5319	1.1534
	0.80	0.4871	0.4882	0.8000	0.6521
P_{g1}	0.20	0.2084	0.2230	0.3285	0.1764
P_{g2}	0.20	0.1180	0.1000	0.3000	0.2052
P_{g3}	0.50	0.2135	0.2157	0.5000	0.4226
P_{g4}	0.20	0.1200	0.1200	0.4000	0.2779
P_{g5}	1.050	1.1000	1.1000 1.0810	1.1000	1.1000
P_{g6}	1.045	1.0877	1.0580	1.0977	1.0885
V_{g1}	1.010	1.0689	1.1000	1.0865	1.0788
V_{g2}	1.050	1.1000	1.0435	1.0230	1.1000
V_{g3}	1.010	1.0613	1.0837	1.0800	1.0515
V_{g4}	1.050	1.1000	0.9840	1.1000	1.0582
V_{g5}	0.978	0.9760	1.0430	1.1000	0.9826
V_{g6}	0.969	1.0512	0.9534	0.9000	0.9590
T_{t1}	0.932	0.9813	0.9667	1.0115	1.0342
T_{t2}	0.968	0.9590	0.1294	0.9841	0.9710
T_{t3}	0	0.0020	0.1487	0.1932	0.1529
T_{t4}	0	0.1425	0.0135	0.1781	0.1817
Q_{c10}	0	0	0.1817	0	0
Q_{c12}	0	0.0493	0.0754	0.1549	0.0593
Q_{c15}	0	0.0431	0	0.0735	0.0626
Q_{c17}	0	0.1040	0.0253	0	0.1266
Q_{c21}	0	0.0252	0.0961	0	0.0203
Q_{c22}	0	0.0291	0.0303	0.1316	0.0399
Q_{c23}	0	0.0228		0.0485	0.0564
Q_{c24}					
Q_{c29}					
Cost($/hr)	900.5995	798.9124	**799.0958**	963.4846	857.6473
Power Loss(p.u.)	0.0533	0.0858	0.0862	**0.0264**	0.0536
Lj2s		0.1154	0.1067	0.1046	**0.1044**
t(s)	0.1456	156.8580	212.3940	254.6390	255.3720

Table 4 Comparison of fuel costs

Method	Base Case	MATPOWER [53]	IPM	GA	EP	PSO	IEP [54]	DE	AuDE
Cost($/h)	900.5995	804.0600	803.986	805.3076	801.1315	800.3484	802.4650	800.2241	798.9124

Table 5a
Number of transmission lines/buses under different severity category before and after optimization without SSSC device

			NLL				NVP			NVS					NQG			FLCC Index
			LS	BS	AS	MS	LS	BS	AS	VLS	LS	BS	AS	MS	LS	BS	AS	
Before Optimization			37	4	0	0	24	0	0	24	0	0	0	0	6	0	0	0697.2519
After Optimization	Without TS Constraints		34	6	1	0	0	0	24	24	0	0	0	0	6	0	0	2968.7000
	With TS Constraints	Cost	33	7	1	0	18	0	6	24	0	0	0	0	6	0	0	1349.5000
		Ploss	35	6	0	0	24	0	0	24	0	0	0	0	5	0	1	0761.1393
		Lj2s	32	9	0	0	5	0	19	24	0	0	0	0	6	0	0	2520.0000

Table 5b
Number of transmission lines/buses under different severity category before and after optimization with SSSC device

			NLL				NVP			NVS					NQG			FLCC Index
			LS	BS	AS	MS	LS	BS	AS	VLS	LS	BS	AS	MS	LS	BS	AS	
Before Optimization			37	4	0	0	24	0	0	24	0	0	0	0	6	0	0	0697.2519
After Optimization	Without TS Constraints		34	6	1	0	0	0	24	24	0	0	0	0	6	0	0	2968.7000
	With TS Constraints	Cost	32	8	1	0	1	0	23	24	0	0	0	0	5	0	1	3006.2000
		Ploss	34	6	1	0	0	0	24	24	0	0	0	0	5	0	1	3059.7000.
		Lj2s	30	11	0	0	0	0	24	24	0	0	0	0	5	0	1	3088.0000

where
NLL=Number of lines/transformers loadings;
NVP=Number of bus voltages
NVS=Number of voltage stability indices
NVQ=Number of generator reactive power outputs

The classification of transmission lines/transformers, load bus voltage profiles, voltage stability indices and generator reactive power outputs under different severity category before optimization and after optimization is given in Table 5 without and with SSSC device respectively. From the Table 5 it can be observed that the number of lines/buses under different severity categories and the FL based severity index are increased after optimization with the proposed AuDE algorithm. The reason behind this is that the numbers of voltage profiles/buses under AS severity category are more after optimization than before optimization.

X. RESULT AND DISCUSSION

The following are the critical problems addressed/issues resolved/contributed in this paper.

1) A new evolutionary algorithm namely adaptive unified differential evolution is developed for solving the TS-OPF problems to meet the pressing needs of the vertically integrated power systems.
2) An OPF problem formulation was made with both voltage stability and transient stability constraints along with various equality and inequality constraints.
3) A maiden attempt has been made to include the SSI as a security level before going to TS assessment.
4) A fuzzy logic based SSI for network contingency ranking method is developed to identify the critical network contingencies.
5) The proposed AuDE algorithm gives the best results without and with SSSC compared to the other methods reported in the literature
6) The presence of SSSC is reducing the little bit cost of generation, power loss and maximum of voltage stability L-index.
7) The SSI based severity indices are increased after optimization which means that the stress on the system has been increased after optimization.
8) From the case studies, it was observed that the proposed AuDE method has achieved good results while on using SSSC device to solve the transient stability and voltage stability constraints included in the OPF problem.
9) Evaluation of transient stability using time-domain simulation is a time consuming process for the proposed AuDE approach based OPF problem. But, when compared to New England 39-bus-10-genertor system, the IEEE 30-bus-6-generator system has shown moderate time consumption.

XI. CONCLUSION

In this paper, a fuzzy logic based SSI for network contingency ranking was presented. Modern power systems pressing needs were addressed using the AuDE method adopting SSSC device to solve the TS-OPF problems. Compared to other past works in literature, the installation of FACTs devices advantages was accurately evaluated by the proposed method. This optimization process has been done using three different objective functions of optimal power flow solutions of formulated large-scale optimization problem. Efficiency of proposed method in determining the optimal solution was validated and tested through analyzing the impacts of FACTs device (e.g. SSSC device). Using 39–bus test systems and IEEE 30–bus systems and the implementation of proposed approach was achieved successfully. Better maintenance of transient stability and low fuel cost solution was the goodness achieved with proposed method when compared to the abilities of other existing methods. Also, the SSSC device is adopted to improve the performance of power system.

REFERENCES

1. Carpentier J., "Optimal power flows", *Int J Electr Power Energy Syst* ;1 (1):3–15, 1979.
2. Dommel HW, and Tinney WF., "Optimal power flow solutions", *IEEE Trans Power Apparat Syst* PAS-87(10):1866–76,1968.
3. Xue Y, Pavella M., "Extended equal-area criterion: an analytical ultra-fast method for transient stability assessment and preventive control of power systems", *Int J Electr Power Energy Syst* 11(2):131–49,1989.
4. Alejandro Pizano-Martínez, Claudio R. Fuerte-Esquivel, and Daniel Ruiz-Vega, "Global transient stability-constrained optimal power flow using an OMIB reference trajectory," *IEEE Trans. Power Syst*, vol. 25, no. 1, pp.392-403, Feb. 2010.
5. Y. Sun, Y. Xinlin, and H. F. Wang, "Approach for optimal power flow with transient stability constraints," *Proc. Inst. Elect. Eng., Gen., Transm., Distrib.*, vol. 151, no. 1, pp. 8–18, Jan. 2004.
6. D. Ruiz-Vega and M. Pavella, "A comprehensive approach to transient stability control. I. Near optimal preventive control," *IEEE Trans. Power Syst*., vol. 18, no. 4, pp. 1446–1453, Nov. 2003.
7. K.karoui, L.platbrood, H. Crisciu, and R. A. Waltz, "new large-scale security constrained optimal power flow program using a new interior point algorithm," 5th international conference, European electricity Market, pp.1-6, 28-30 May 2008.
8. A A. Fouad and T. Jianzhong, "Stability constrained optimal rescheduling of generation," *IEEE Trans. Power Syst*., vol. 8, no. 1, pp. 105–112, Feb. 1993.
9. A. L. Bettiol, L. Wehenkel, and M. Pavella, "Transient stability-constrained maximum allowable transfer," *IEEE Trans. Power Syst*., vol. 14, no. 2, pp. 654–659, May 1999.
10. Yan Sun and Thomas J. Overbye "Visualization for power system Contingency analysis data," IEEE transactions on power systems, Vol.19, No. 4, pp.1859-1866, November 2004.
11. Xia Y, Chan KW, Liu M., "Direct nonlinear primal-dual interior-point method for transient stability constrained optimal power flow," *IEE Proc Gener Transm Distrib* 152(1):11–6, 2005.
12. Jiang Q, Geng G., "A reduced-space interior point method for transient stability constrained optimal power flow," *IEEE Trans Power Syst* 25(3):1232–40, 2010.
13. Jiang Q, Huang Z., "An enhanced numerical discretization method for transient stability constrained optimal power flow," *IEEE Trans Power Syst* 25 (4):1790–7, 2010.
14. Pizano-Martinez A, Fuerte-Esquivel CR, Ruiz-Vega D., "A new practical approach to transient stability-constrained optimal power flow," *IEEE Trans Power Syst* 2011;26(3):1686–96, 2011.
15. Xu Y, Dong ZY, Meng K, et al., "A hybrid method for transient stability constrained optimal power flow computation*," IEEE Trans Power Syst* 27 (4):1769–77, 2012.
16. Geng G, Jiang Q., "A two-level parallel decomposition approach for transient stability constrained optimal power flow," *IEEE Trans Power Syst* 27(4):2063–73, 2012.
17. Tangpatiphan K, Yokoyama A., "Adaptive evolutionary programming with neural network for transient stability constrained optimal power flow," *Proc 15th int conf on intelligent system applications to power systems* (ISAP '09), Curitiba, November 8–12. p. 1–6, 2009.
18. Aparajita Mukherjee, Provas Kumar Roy, and V. Mukherjee, "Transient stability constrained optimal power flow using oppositional krill herd algorithm", *Electrical Power and Energy Systems*,83 283–297, (2016). .
19. Rautray SK, Choudhury S, Mishra S, et al., "A particle swarm optimization based approach for power system transient stability enhancement with TCSC", *Procedia Technol* 6:31–8,2012.
20. Joel R Sutter , John N Nderu and Christopher M Muriithi, "Power system oscillations damping and transient stability enhancement with application of SSSC FACTS devices ", *European Journal of Advances in Engineering and Technology*, 2(11): 73-79, 2015..
21. Chan KY, Ling SH, Chan KW, Iu HHC, and Pong GTY., "Solving multi-contingency transient stability constrained optimal power flow problems with an improved GA," *IEEE congress on evolutionary computation*; p. 2901–8,2007.

22. Mo N, Zou ZY, Chan KW, and Pong TYG., "Transient stability constrained optimal power flow using particle swarm optimization," *IET Proc Gener Transm Distrib* 1(3):476–83,2007.
23. Cai HR, Chung CY, Wong KP. Application of differential evolution algorithm for transient stability constrained optimal power flow. *IEEE Trans Power Syst* ;23(2):719–28, 2008.
24. Rainer Storn and Kenneth Price, "Differential evolution – a simple and efficient heuristic for global optimization over continuous spaces," *Journal of Global Optimization* 11: 341–359, 1997
25. J. Vesterstrom ; R. Thomsen, A comparative study of differential evolution, particle swarm optimization, and evolutionary algorithms on numerical benchmark problems," *Proceedings of the Congress on Evolutionary Computation* (IEEE Cat. No.04TH8753), 19-23 June 2004.
26. F. Neri and V. Tirronen, "Recent advances in differential evolution: a survey 285 and experimental analysis," Artif. Intell. Rev. 33, p. 61, 2010.
27. K. Price and R. Storn, "Minimizeing the real functions of the ICEC'96 contest by differential evolution," *IEEE International Conference on Evolutionary Computation*, 1996, pp.842-844..
28. P. Kessel, and H. Glavitsch, "Estimating the voltage stability of a power system," *IEEE Transactions on Power Delivery* PER-6(3):346 – 354, August 1986
29. N. Yorino, E. E. El-Araby, H. Sasaki, and S. Harada, "A new formulation for FACTS allocation for security enhancement against voltage collapse," *IEEE Trans. Power Syst.*, vol. 18, no. 1, pp. 3–10, Feb. 2003.
30. M. Eghbal, N. Yorino, E. E. El-Araby, and Y. Zoka, "Multi load level reactive power planning considering slow and fast VAR devices by means of particle swarm optimization," *IET Trans. Gen., Transm., Distrib.*, vol. 2, no. 5, pp. 743–751, 2008.
31. R. Zárate-Miñano, A. J. Conejo, and F. Milano, "OPF-Based security re-dispatching including FACTS devices," *IET Trans. Gen., Transm., Distrib.*, vol. 2, no. 6, pp. 821–833, 2008.
32. G. N. Taranto, L. M. V. G. Pinto, and M. V. F. Pereira, "Representation of FACTS devices in power system economic dispatch," *IEEE Trans. Power Syst.*, vol. 7, no. 2, pp. 572–576, May 1992.
33. X.P.Zhang, 'Advanced modelling of multi-control functional static synchronous series compensator (SSSC) in Newton-Raphson power flow', *IEEE Trans.Power Syst.*18(4), 1410-1416, 2003.
34. Ghadir Radman, Reshma S. Raje, 'Power flow model/calculation for power systems with multiple FACTS controllers', *Electric Power Systems Research* 77, 1521-1531, 2007.
35. Enrique Acha, Claudio R. Fuerte-Esquivel , Hugo Ambriz-Pérez , César Angeles-Camacho, "FACTS: Modelling and Simulation in Power Networks ," *Wiley*, ISBN: 978-0-470-85271-2, pages.420 February 2004.
36. Thukaram Dhadbanjan, Lawrence Jenkins, H.P. Khincha, **B. Ravikumar** and K.Visakha", Fuzzy logic application for network contingency ranking using composite criteria", *International journal of engineering intelligent systems for electrical engineering and communications* 15(4):205-212
37. Storn R (1996b), "On the usage of differential evolution for function optimization", *Proceedings of the IEEE biennial conference of the North American fuzzy information processing society*, pp 519-523.
38. E. Mezura-Montes, J. Velazquez-Reyes, and C. A. Coello Coello, "A comparative study of differential evolution variants for global optimization," pp. 485- 492.1996
39. K. Price and R. Storn, "Minimizing the real functions of the ICEC'96 contest by differential evolution," *IEEE International Conference on Evolutionary Computation*, pp.842-844,1996.
40. Q. K. Pan, P. N. Suganthan, L. Wang, L. Gao, and R. Mallipeddi, "A 315 differential evolution algorithm with self-adapting strategy and control parameters," *Computers & Operations Research*, vol. 38, no. 1, pp. 394-408, 2011.
41. A. K. Qin, V. L. Huang, and P. N. Suganthan, "Differential evolution algorithm with strategy adaptation for global numerical optimization," *IEEE Transactions on Evolutionary Computation*, vol. 13, no. 2, pp. 398-417, 2009.
42. Y. Wang, Z. Cai, Q. Zhang, "Differential evolution with composite trial vector generation strategies and control parameters," *IEEE transactions on Evolutionary Computation*, vol. 15, no.1, p. 55, 2011.
43. K. V. Price, "An introduction to differential evolution," New Ideas in Optimization, *D. Corne, M. Dorigo, and V. Glover, Eds.* London, U.K.: McGraw-Hill, pp. 79-108. 305, 1999.
44. M. M. Ali and A. Torn, "Population set based global optimization algorithms: Some modifications and numerical studies," *Comput. Oper. Res.*, vol. 31, no. 10, pp. 1703-1725, 2004.
45. J. Brest, S. Greiner, B. Bovskovic, M. Mernik, and V. Zumer, "Self adapting control parameters in differential evolution: A comparative study on numerical benchmark problems," *IEEE Transactions on Evolutionary Computation*, vol. 10, no. 6, pp. 646-657, 2006.
46. J. Zhang and A. C. Sanderson, "JADE: adaptive differential evolution with optional external archive," *IEEE Transactions on Evolutionary Computation*, vol. 13, no. 5, pp. 945-958, 2009.
47. J. Liu and J. Lampinen, "A fuzzy adaptive differential evolution algorithm," *Soft Computing, A Fusion of Foundations, Methodologies and Applications*, vol. 9, no. 6, pp. 448-642, 2005.
48. W. Gong, Z. Cai, C. X. Ling, and H. Li, "Enhanced differential evolution with adaptive strategies for numerical optimization," *IEEE Transactions on Systems, Man, and Cybernetics - Part B*, vol. 41, no. 2, pp. 397-413, 2011.
49. D. Corne, M. Dorigo, and F. Glover, New ideas in optimization, London, U.K.:*McGraw-Hill Education*, 102,1999.
50. Giovanni Iacca, Ferrante Neri, and Ernesto Mininno, "Opposition-Based Learning in Compact Differential Evolution", *European Conference on the Applications of Evolutionary Computation Evo Applications* 2011: Applications of Evolutionary Computation pp 264-273.
51. O. Alsac and B.Stott "Optimal load flow with steady state security", *IEEE PES Summer Meeting and EHV/UHV Conference*, Vancouver, Canada, T73 484-3.
52. S. Kalyani and K. Shanti Swarup, " Study of neural network models for security assessment in power systems", International Journal of Research and Reviews in Applied Sciences, Vol. 1, Issue 2, , pp. 104-117, November 2009.
53. R. D. Zimmerman and D. Gan, "MATPOWER, a MATLAB power system simulation package," *Power System Engineering Research Center*, Cornell Univ., Ithaca, NY, 1997. [Online]. Available: http://www.pserc.cornell.edu/Matpower.
54. A. A. Fouad and V. Vittal, "Power system transient stability analysis using the transient energy function method*", Englewood Cliffs*, NJ: Prentice-Hall, 1992.
55. T. Nguyen and M. A. Pai, "Dynamic security-constrained rescheduling of power systems using trajectory sensitivities," *IEEE Trans. Power Syst.*, vol. 18, no. 2, pp. 848–854, May 2003.

AUTHORS PROFILE

B. Venkateswarlu received the B.E Electrical Engineering degree from the college of Engineering, Osmania University Hyderabad in 1993, Telegana, India, M.Tech degree from college of Engg JNTU Anantapur, AP, India in 2006. He is currently pursuing the Ph.d from JNTU, Anantapuramu. Presently he is working as the Head of Electrical and Electronics Engineering at Government .Polytechnic, Proddatur, Kadapa, A.P.,India. His research interests include power system planning, operation, FACTS controllers and power system optimization

K. Vaisakh (M'06) received the B.E. degree in electrical engineering from Osmania University, Hyderabad, India, in 1994, the M.Tech. degree from JNT University, Hyderabad, India, in 1999, and the Ph.D. degree in electrical engineering from the Indian Institute of Science, Bangalore, India, in 2005. Currently, he is a Professor with the Department of Electrical Engineering, AU College of engineering, Andhra University, Visakhapatnam, India. He has published more than 125 papers in reputed journals and has been serving as an editorial board member of reputed international journals. His research interests include optimal operation of power system, voltage stability, FACTS, power electronic drives, power system dynamics, power system optimization, and control.